Magnetically geared propulsion motors

Stuart Calverley[1], Harry Wood[2],
David Powell[3] and Radu-Stefan Dragan[3]
[1]Chief Engineer, Magnomatics Ltd, Sheffield, UK
[2]Design Engineer, Magnomatics Ltd, Sheffield, UK
[3]Principal Engineer, Magnomatics Ltd, Sheffield, UK

Abstract — The paper describes a new type of propulsion system using an electrical drive with transmission through a hermetically sealed magnetic gear unit. The design requirements of the system are presented, and a parametric approach to optimisation is discussed, where features such as system mass, cost and efficiency can be analysed.

1 Introduction

The use of electrical machines to provide underwater propulsion presents the user with a series of operational advantages. Precise speed control with high transient capability can offer significant benefits in many applications, especially those challenged with keeping station. However, the systems also present a set of challenges to the designer. The motors must be sealed against seawater to provide the electrical integrity and corrosion protection, and often the motors themselves are oil filled to provide pressure compensation. The longevity, integrity and reliability of the motor is therefore intrinsically linked to that of the shaft seal which allows the rotating shaft access to the propulsor. Failure of the seal leads to the ingress of seawater and the outflow of oil. The secondary challenge arises from the need to match the propeller speed requirements, which favour low speed, with those of the electric motor which favours high speed to deliver a specified power at relatively low torque and therefore size.

2 Approach

To eliminate the need for a shaft seal a motor system incorporating a new type of magnetic gear coupling is used. The high torque density magnetic gear is described in [1, 2, and 3]. In these gear systems the torque is transmitted using a magnetic interaction between two arrays of magnets of different pole numbers facing each other across an intermediate ring of ferromagnetic pole pieces.

The magnetic gear has analogies with an epicyclic gear. Figure 1 shows a schematic of a magnetic gear with the epicyclic analogy for reference. The inner rotor is the high-speed element of the system and in this case is connected directly to the drive motor. The outer rotor (or ring gear) is the low speed, high torque output and is connected to the propeller. The array of planets in the mechanical gear is replaced, in the magnetic system by a stationary array of steel “pole pieces” that are set within a glass fibre structure that also serves as the isolating membrane. These pole pieces modulate the magnetic fields of the inner and outer rotors give a gear ratio between the motor and propeller shafts.

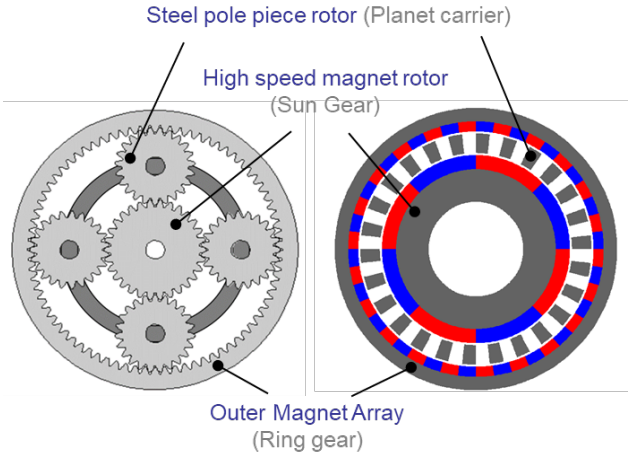

Figure 1. Mechanical and magnetic gear analogies.

Since this gear system is a magnetic device there are many ways with which this system can be integrated with a motor drive system. In one example the electromagnetic nature of the gear can be exploited to create an electronically controlled continuously variable transmission [4], while integrating the gear into the core of a high-speed brushless permanent magnet machine gives extraordinarily high prime-mover torque output in a so-called pseudo-direct drive motor [5]

In this case however a more rudimentary system is used. The key objective is to transmit the motor power from within the thruster magnetically without the use of a rotating shaft seal. In this case the motor and gear are not integrated but laid out in a more conventional motor-gearbox arrangement. The use of this magnetically geared system in this manner presents two key technical advantages. Firstly, the geared system allows the motor to

operate at a higher speed than the propeller, this reduces the torque burden on the electrical machine and leads to a proportionate reduction in motor size and hence, with reduced diameter, the hydrodynamic efficiency of the propulsor is maximised. Secondly the specific features of a magnetic gear allow for torque transmission through a separating membrane that becomes an integral part of the magnetic circuit, and hence the through-wall transmission does not have a detrimental effect on the overall torque transmission capability.

2.1 Geared, sealed system

The complete system comprises a high-speed electrical machine that is coupled to the input shaft of a magnetic gear in an oil filled, pressure compensated chamber. The magnetic gear comprises a stationary element within which an array of steel pole pieces is included. These pole pieces are embedded in a glass fibre retention system which, as discussed, acts as a non-permeable barrier. Torque is transmitted through the barrier, and at the same time the rotational speed is geared down and torque increased. This has the added benefit that high-speed electrical machines are more power-dense and therefore much smaller than their non-geared, direct drive counterparts. Finally, the high-torque, low-speed rotor of the magnetic gear is connected to the propulsor on the seawater side of the system.

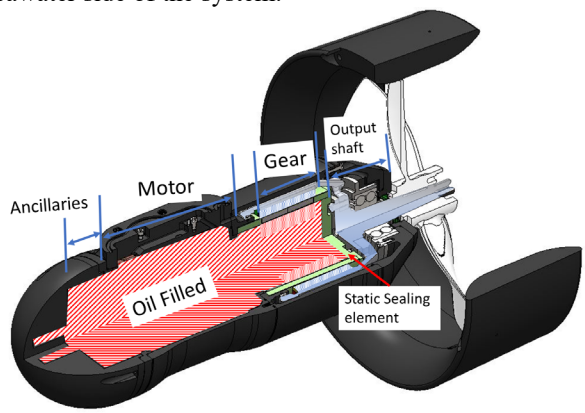

Figure 2. Cut away section of motor showing key components and hermetic sealing arrangement.

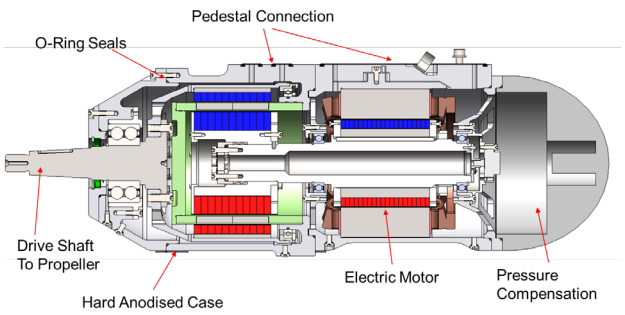

Figure 3. Section of propulsion system

Combining the system in this way gives the designer many degrees of freedom and, given the complexity of the application a design procedure is defined to aid the optimisation.

3 Design

At the early design stage the key design feature that must be addressed at the outset is the gear ratio. High gear ratios lead to a smaller, lower cost, drive motor, however the increased rotational speeds give rise to increasingly significant drag losses in the oil as it shears in the narrow gap between the rotor and stator. The decision is also moderated by the effectiveness of the magnetic gear at different ratios. For magnetic gears single stages between 3:1 and 7:1 lead to the most compact designs, however, in this case the analysis of gear ratios was restricted to values between 2:1 and 4:1 due to the rapid rate at which oil viscous drag increases with prime mover speed.

3.1 Electromagnetic design

To address the fundamental aspect of gear ratio and accommodate all the disparate design features that influence the system a comprehensive design study was undertaken to establish representative gear designs. In this case a parametric approach was undertaken, where key variables such as, for example, pole numbers and geometric variables such as magnet dimensions were varied, and each combination resulted in a model that was analysed using the finite element method. In total approximately 16,000 designs with 3, 4, 5 and 6 pole-pair rotors spanning gear ratios between 2.33:1 and 3.5:1 were analysed in this way. Example output for 5 pole-pair rotor variants is shown in Figure 4, where each dot represents a specific design.(note that 3pxx is shorthand for 3.xx:1 gear ratio)

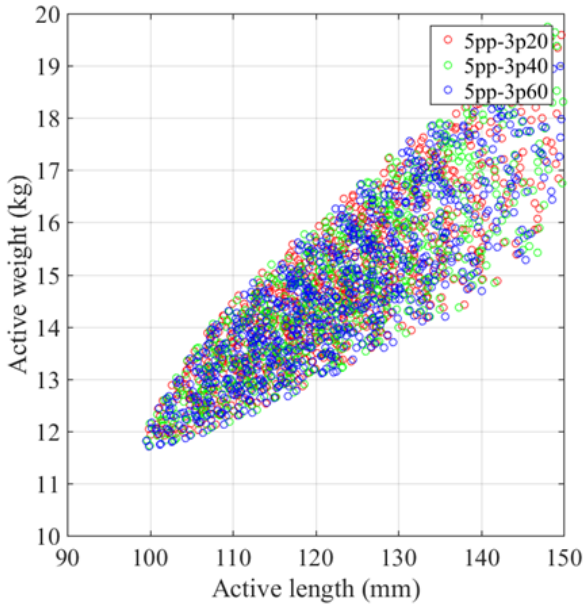

Figure 4. Example output from parametric design sweep showing variation between component weight and required active length.

The process is repeated for all the rotor pole combinations mentioned and two example 3 pole pair, 4.33:1 designs are shown in Figure 5 and Figure 6 respectively. The design in Figure 5 has an outer diameter of 180mm and relatively thin magnets, whilst the design in Figure 6 has a larger diameter of 200mm and relatively thick magnets. Given the lower magnet thickness and diameter, the design of Figure 5 may be initially considered to give a more cost effective solution, however the lower magnet thickness reduces the torque producing capability of this example by 46% when compared to that of Figure 6. Hence the lower magnet thickness design leads to an increase in axial length and gear mass of 85% and 72% and counterintuitively, to deliver the same torque requires an additional 1.3% magnet mass.

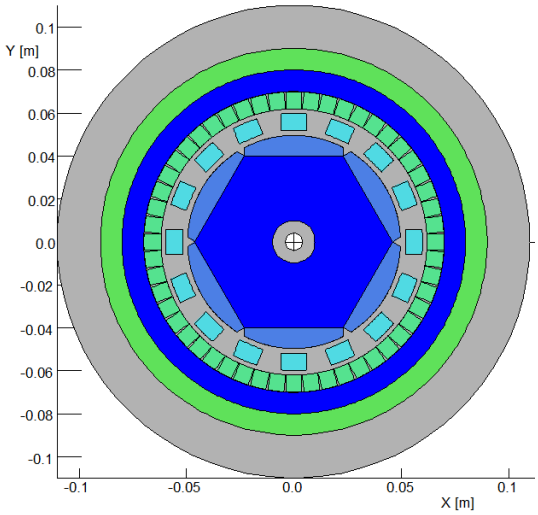

Figure 5. Example 3 pole pair, 4.33:1 magnetic gear with OD of 180mm.

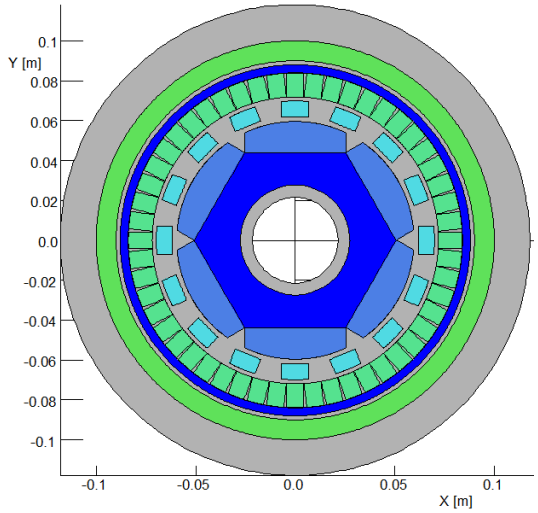

Figure 6. Example 3 pole pair, 4.33:1 magnetic gear with OD of 200mm.

It is apparent that the use of a sequential design process can lead to counterintuitive results and to facilitate an optimisation process a cost function is applied to a material mass breakdown. This function is used for each pole number considered and a geometrically optimised design was recorded from the data set of Figure 4 and the corresponding sets for other pole combinations. The mass of the cost optimised designs is shown in Figure 7, where the benefits of increased gear ratio are immediately apparent and significant savings are accrued even at the modest gear ratios analysed.

When considering the efficiency of these designs the major loss contributor is the viscous drag of the oil which increases rapidly as gear ratio is increased and leads to a marked decrease in overall expected efficiency. This critical design aspect is treated separately in the following sections.

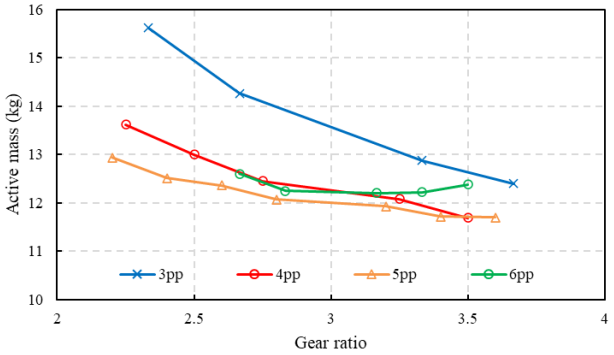

Figure 7. Active mass of gear vs gear ratio for lowest cost variants

3.2 Oil drag consideration

The viscous drag of the oil filled system plays perhaps the most significant role in the optimisation. For many electrically driven systems there are cost and size advantages of using a system with a high gear ratio. This allows the drive motor to operate at high speed with a low torque requirement, driving down the size and cost of this high value element. In this underwater application the optimisation is heavily influenced by the secondary requirements of the system since:

1) The motor is pressure balanced and hence oil-filled and viscous drag losses become highly significant in high speed systems with relatively narrow gaps.
2) The relative cost of power, whether in a battery or tethered system is high. Recharging or providing cables to the depths discussed presents a significant cost to the operation which is increased by electrical inefficiency of the motor.

When examining the relationship between the viscous drag and the motor speed/gear ratio there is a further relationship that seeks to complicate the optimisation. As the motor speed is increased (using the gear ratio) the size of the motor is reduced and the radial length of the airgap (which is primarily a function of tolerance accommodation) does not significantly change, hence the viscous drag does not rise as fast with gear ratio as a parameter-based analytical approach would suggest.

At this early stage of design there is a requirement therefore to provide a computationally efficient model to calculate viscous drag loss that can be applied to a data set of similar size to that presented in Figure 4. The model presented by Bilgen and Boulos [1] was selected as this satisfies the requirement to accommodate specific geometric features and hence this can be included into the early stage design scan process.

By including the anticipated drag loss into the design output an initial estimate of gear efficiency can be included in the optimisation. Since the gear ratio affects the speed of the entire high speed rotating shaft system, including that associated with the drive motor, the viscous drag presented also includes drag associated with the entire high speed shaft system. The gear efficiencies (including total viscous drag) of the cost optimised designs discussed are shown in Figure 8 where the anticipated reduction is apparent at increased gear ratio.

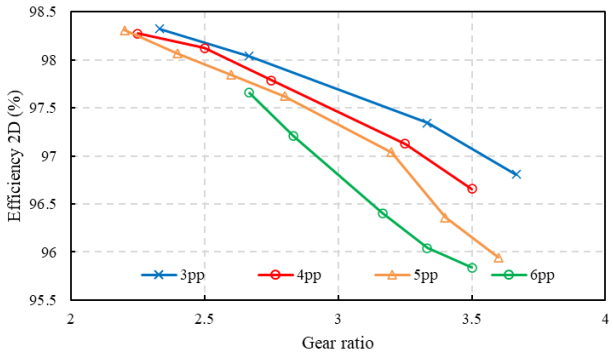

Figure 8. Gear efficiency (including total system viscous drag losses) vs gear ratio for lowest cost variants.

3.3 Oil drag testing

Since the oil drag represents the most significant loss mechanism in the system and has arguably the lowest calculation confidence level for all the losses considered this parameter was independently experimentally validated. A dummy machine was constructed (shown in Figure 9) with replica oil shear regions and internal cartridge heaters representing the losses and heating effect of the motor windings, to allow the oil to be heated to representative conditions. To replicate the submerged environment the dummy machine was water cooled and a flow of 6.5l/min was applied to the cooling jacket to represent the flow of sea water in an operational thruster. The dummy rotor system was operated externally using a dynamometer drive and torque was measured using an inline torque transducer. Component and fluid temperatures were monitored throughout the testing using thermocouples.

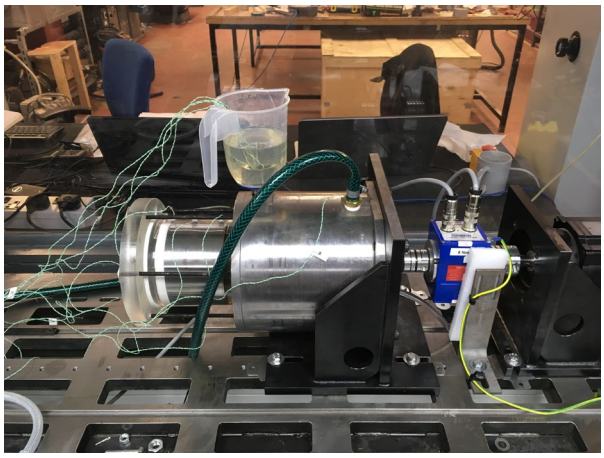

Figure 9. Dummy rotor system for oil drag testing

The rotor was spun at the desired speed using the external dynamometer drive which requires a dynamic shaft seal on the oil filled system. To determine the magnitude of drag on this seal a series of tests were performed with and without the oil in the system. For the oil filled tests the system was operated until thermal equilibrium was achieved where it must be noted that the operating temperature was relatively low since other system losses are not present. In this low temperature case the oil viscosity is relatively high and the total measured drag is considerably higher than is expected in an operational system. The Bilgen and Boulos viscous drag model discussed was applied to calculate viscous drag losses in the relatively cold oil and the thermal behaviour of the oil and corresponding changes in viscosity were not included in the analytical methods. The comparison between the experimental results (with dynamic seal drag torque subtracted) and the analytical model are shown in Figure 10. The results show good agreement between the measured and predicted values where a deviation is noted at the highest speed which is attributed to a temperature increase in the oil at these higher loss values.

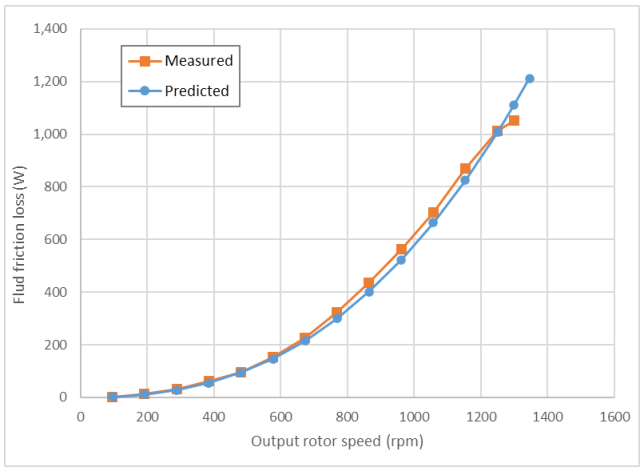

Figure 10. Measured and predicted oil drag in the dummy machine system in cold oil

The dummy machine system included a series of cartridge heaters to replicate the heating effect of the losses in the windings of the drive machine. The usage of the system was therefore expanded which allowed operation to validate thermal models and cooling systems of a loaded

machine. The system was operated with an additional heat input of 1250W into the cartridge heaters, which represents the thermal load at the full rated power of the system. Figure 11 shows a graph of the oil temperatures recorded in the airgap region at the Non-Drive End (NDE) and Drive End (DE) of the system as well as that adjacent to the mid axial section of the cartridge heater (representing the winding). The system includes provision for axial oil flow to prevent "hot spots" and it is apparent that the oil is warmed by the viscous drag losses as it passes through the airgap from the drive end to the non-drive end. At 2500s the thermal load was increased to 1592W which represents the value at 125% overload condition. For the full rated power case the maximum oil temperature was 55°C, which increased to approximately 60°C during the overload condition. These values gave an acceptable overhead against the maximum specified temperature in this application.

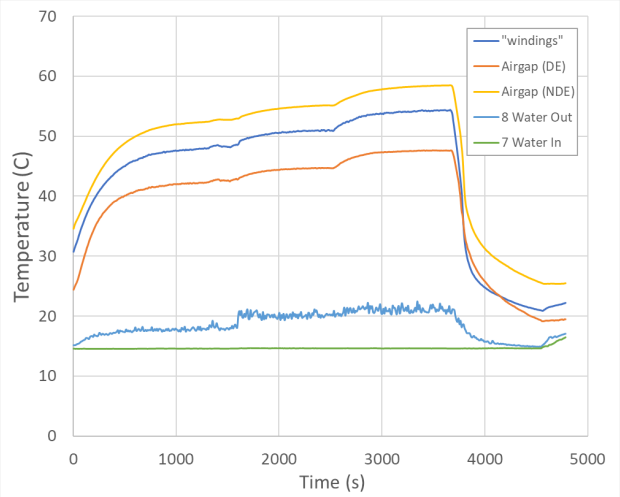

Figure 11. Selected temperatures recorded in dummy system with additional thermal input representing losses in the motor

4 Final machines

The machines are manufactured at Magnomatics and tested using a purpose built flooded dynamometer system. Figure 12 shows a pole piece array embedded within the glass fibre structure before being inserted into the gear housing and Figure 13 shows a final drive rotor with magnet array.

Figure 12. Sealing pole piece array before insertion into gear casing.

Figure 13. Magnetic gear final drive rotor

5 Thrusters

Using this design process two motor and gear systems have been developed at 15kW and 25kW ratings respectively. The transmissions are mated to the corresponding thrusters and the completed propulsor is shown in Figure 14. with headline specifications for the units shown in Table 1

Figure 14. Complete 25kW thruster (courtesy SMD).

Table 1. Headline thruster specifications

	15kW	**25kW**
Rated speed	1600rpm	1300rpm
Rated torque	100Nm	185Nm
Thrust	350kgf	540kgf
Weight in air*	52kg	80kg
Weight in water*	34kg	44kg
Length*	660mm	759mm
Width*	462mm	557mm
Prop diameter	330mm	390mm
Input voltage	680VDC	
Depth rating	6000m	
Temperature (operating)	-10°C to 45°C	

*Complete thruster

The thrusters have undergone extensive tank testing with more than 100,000 fault-free accelerated aging full to zero power cycles and are currently operational in ROV systems with a depth rating of 6000m.

6 Conclusions

The motors present a new type of propulsion system enabled by the magnetic gear. A design process is shown which aims to balance the often competing needs of the gear ratio selection to give an optimised size, weight and cost with acceptable increases in viscous drag caused by the pressure compensating oil-filled system. The deletion of the dynamic shaft seal minimises the probability of harmful transformer oil spills, minimises the service requirements and greatly increases the reliability of the system by preventing the ingress of seawater.

7 Acknowledgements

The systems described were designed by Magnomatics Limited in partnership with Soil Machine Dynamics Limited for use in their range of electrically powered remotely operated vehicles. The authors are grateful for the continued support of SMD and permission to reproduce data in this publication.

8 References

[1] Atallah, K. Calverley, S. D. Howe, D. ‘High performance magnetic gears’ Journal of Magnetism and Magnetic Materials, Vols 272-276 (1), ppE1727-E1729, May 2004.
[2] Tallerico, T. F., Scheidler J. J , and Cameron, A. A., . ‘Electromagnetic mass and efficiency of magnetic gears for electrified aircraft.’ 2019 AIAA/IEEE Electric Aircraft Technologies Symposium (EATS). IEEE, 2019.
[3] Bird JZ. ‘A Review of Electric Aircraft Drivetrain Motor Technology.’ IEEE transactions on magnetics. Vol 58 (2):pp1–8 2022;.
[4] Atallah K, Wang J, Calverley SD, Duggan S. ‘Design and Operation of a Magnetic Continuously Variable Transmission’. IEEE transactions on industry applications. 2012;48(4):1288–95.
[5] Atallah, K. et al. ‘A Novel "Pseudo" Direct-Drive Brushless Permanent Magnet Machine’, IEEE transactions on magnetics, Vol 44 (11), pp. 4349–4352. 2008.
[6] Bilgen, E. and Boulos, R. (1973) ‘Functional Dependence of Torque Coefficient of Coaxial Cylinders on Gap Width and Reynolds Numbers’, Journal of fluids engineering, Vol 95(1), pp. 122–126. 1973.